

# Oxygen Reduction Reaction Induced pH-Responsive Chemo-Mechanical Hydrogel Actuators

*Cunjiang Yu*<sup>a,\*</sup>, *Peixi Yuan*<sup>b,\*</sup>, *Evan M. Erickson*<sup>b</sup>, *Christopher M. Daly*<sup>b</sup>, *John A. Rogers*<sup>1,a</sup>  
and *Ralph G. Nuzzo*<sup>1,b</sup>

<sup>a</sup> Department of Materials Science and Engineering, University of Illinois-Urbana Champaign,  
Urbana, Illinois 61801

<sup>b</sup> School of Chemical Sciences, University of Illinois-Urbana Champaign, Urbana, Illinois 61801

## **Supporting Information:**

List of content:

- I. CV of the ORR and the adaption of 2-electrode system
- II. Fabrication of serpentine wire mesh for integration in the macro PAA actuator
- III. A single cycle ORR application in micro PAA actuator
- IV. Images of the micro PAA actuator from control experiments
- V. Current density in micro and macro PAA actuators
- VI. Control group of macro-scale PAAm gel
- VII. Supplementary Information figures
- VIII. Supplementary Information movie captions

---

\* *Equal Contribution.*

<sup>1</sup> *Corresponding author, E-mail: [r-nuzzo@illinois.edu](mailto:r-nuzzo@illinois.edu), [jrogers@illinois.edu](mailto:jrogers@illinois.edu).*

## **I. CV of the ORR and the adaption of 2-electrode system**

Fig. S1 shows the cyclic voltammogram (CV) of a 2-electrode system using the Au anode as a pseudo-reference electrode, and the 3-electrode system using Ag/AgCl as a standard reference electrode. The CV was obtained at a scanning rate of 20 mV/Sec. The CV using the Au pseudo-reference electrode is approximately the same as the CV utilizing a Ag/AgCl reference electrode, with potential downshift of 0.95 V, indicating the stability of the Au reference electrode for use as a pseudo-reference electrode in our devices. As shown in the plot, the ORR peak occurs at -0.2 V (Vs. Ag/AgCl) in the 3 electrode system, and at -1.15 V (vs. Au). Hence, for all the experiments across this study we apply -1.15 V at the system for ORR to occur in the 2-electrode system, and we also obtain a current magnitude of 6  $\mu$ A.

## **II. Fabrication of serpentine wire mesh for integration in the macro PAA actuator**

Fig. 2a illustrates the major steps for the integration process of the electrodes and the hydrogel. Specifically, a 2.5  $\mu$ m thick layer of PI was spin coated onto a temporary supporting glass slide, followed by curing at 250 °C and surface treatment by oxygen plasma (March RIE, Plasma Thermal) to ensure better adhesion. Metals of 5 nm thick Cr and 400 nm thick Au were successively evaporated (electron beam evaporation). After patterning the Cr/Au in wet etchants after standard photolithography, and removing the photoresist, another layer of 2.5  $\mu$ m thick PI was spin coated to cover the whole metal layers for future electrode isolation. A thin layer of SiO<sub>2</sub> was then deposited by Plasma Enhanced Chemical Vapor Deposition (PECVD), and selectively opened in Reactive Ion Etching (RIE) (Plasma thermal) by using PR AZ 5214 as mask. The uncovered PI was etched away in oxygen plasma to expose the metal region for the purpose of ORR testing. After removing the masking SiO<sub>2</sub> layer in Buffer Oxide Etchant (BOE),

another 150 nm thick SiO<sub>2</sub> was then deposited by PECVD. The SiO<sub>2</sub> was patterned in RIE using the same approach. The electrode mesh was completed by patterning the two layers of PIs in oxygen plasma, using the patterned SiO<sub>2</sub> as etching mask and followed by removing the top SiO<sub>2</sub> in BOE (See Fig. S2).

In order to apply electrical potentials, electrical connection with wire out is required. The interconnection was performed before embedding the electrode meshes into the PAA hydrogel, since the process occurs at high temperatures. To form electrical contact, anisotropic conductive films (ACF, Elform Heat Seal Connectors), with the form of ribbon cables, were attached to the pads of the meshes at one end and the printed circuit board (PCB) at the other. The films were cured in an oven at 170 °C for 20 minutes to form a solid electrical connection to provide a means for external connections. The electrode mesh with bonded ACF cable was released from the glass substrate by immersion into a buffered oxide etchant (BOE 6:1 diluted) and cleaned in deionized water. Finally, the joint of bonded pad and ACF cable was encapsulated with PDMS in order to avoid any electrical leakage in liquid solution.

### **III. A single cycle ORR application in micro PAA actuator.**

In this experiment, we applied ORR until we observed a plateau in strain change, then removed the ORR, and observed it until full recovery. As shown in Fig. S3, the PAA gel reaches maximum strain change, around 40%, after 30 minutes application of ORR. This result is consistent with previous study of the pH-responsive PAA micro gels<sup>1</sup>. After the ORR was removed for 30 minutes, the gel only recovered to about 90% of its original dimension, a full recovery was achieved at 120 minutes. Since the rate of de-swelling is controlled by the osmotic force to drive water out of the polymer matrix, the de-swelling rate is directly related to the rate

of de-ionization of the PAA polymer chain. It is well observed in previous studies that the de-swelling rate is slower than the swelling rate<sup>1</sup>. Herein, 30 mins was chosen as the time to apply ORR, and 120 mins was chosen as the recovery time for all the experiments across this study.

#### **IV. Images of the micro PAA actuator from control experiments.**

Fig. S4-5 shows the images of PAA micro stripe volume changes with varied electrode distance and current magnitude. In each column, it shows the stripe before application of ORR at 0 min reaction time, just after ORR was stopped at 30 min reaction time, and the final relaxed state at 150 min reaction time.

Fig. S4 shows the change of PAA micro stripes with a fixed gel size (400  $\mu\text{m}$ ) and current magnitude (6  $\mu\text{A}$ ) with a varied electrode distance: 3 mm (Fig. S4a), 6 mm (Fig. S4b), and 12 mm (Fig. S4c). Finally, Fig. S5 shows the change of PAA micro stripes with a fixed gel size (400  $\mu\text{m}$ ) and electrode distance (3 mm) with a varied current magnitude: 3  $\mu\text{A}$  (Fig. S5a), 6  $\mu\text{A}$  (Fig. S5b), and 12  $\mu\text{A}$  (Fig. S5c).

#### **V. Current Density in Micro and Macro PAA actuators**

In order to apply comparable electrochemical conditions we calculated the current density in micro and macro scaled PAA actuators:

$$J = \frac{I}{A} \quad (\text{Eq. S1}),$$

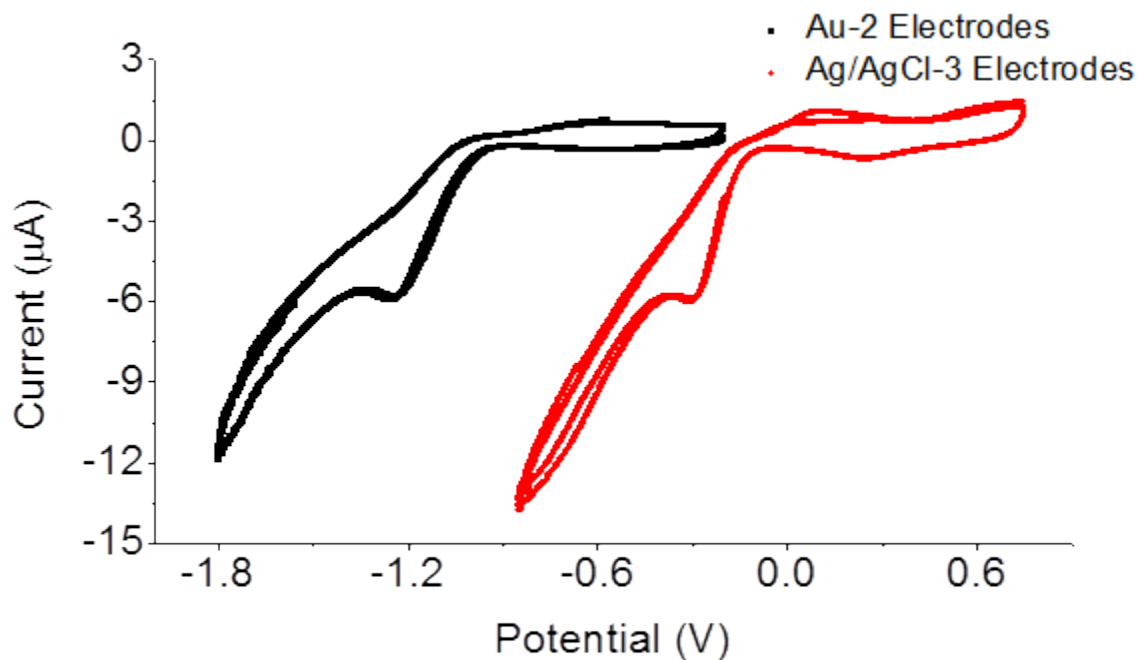
where J is the current density, I is the current magnitude, and A is the effective surface area of the electrode.

In the microscaled electrode, the cathode has two parts: the end of the cathode (0.75 mm x 3 mm) and the top half of the cathode (0.45 mm × 4.5 mm). Only the portion that is immersed in the electrolyte is considered as part of the electrode. The two parts of the cathode yield a total effective electrode surface area of 4.275 mm<sup>2</sup>, and, under a standard 6 μA current magnitude, the microscaled PAA actuator experiences a current density  $J_{micro}=1.40 \mu\text{A}/\text{mm}^2$ . In the macroscaled electrodes, there are 4 chains of stretchable electrodes. In each electrode, there were 18 half circular arcs with the following dimensions: outer radius R=0.28 mm, inner radius r=0.22 mm. The total effective cathode surface area is 3.39 mm<sup>2</sup>, under the 6 μA current, the macroscaled PAA actuator has a current density  $J_{macro}=1.77 \mu\text{A}/\text{mm}^2$ . These results mean that in both micro and macro actuators, the current densities are comparable, which illustrate that the data in both experiments are comparable.

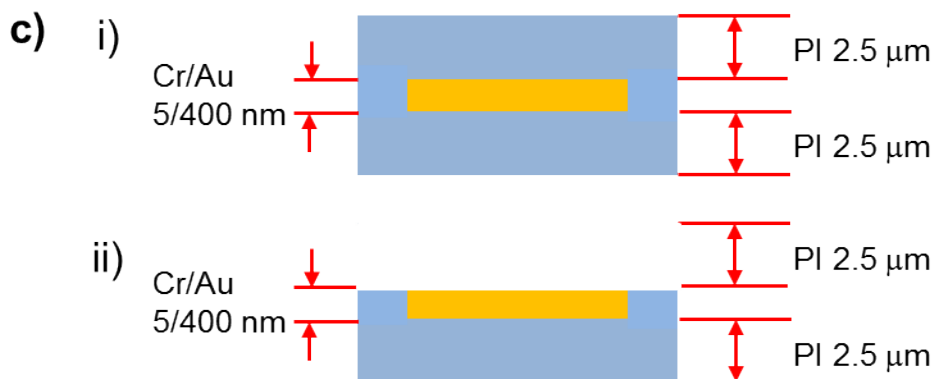
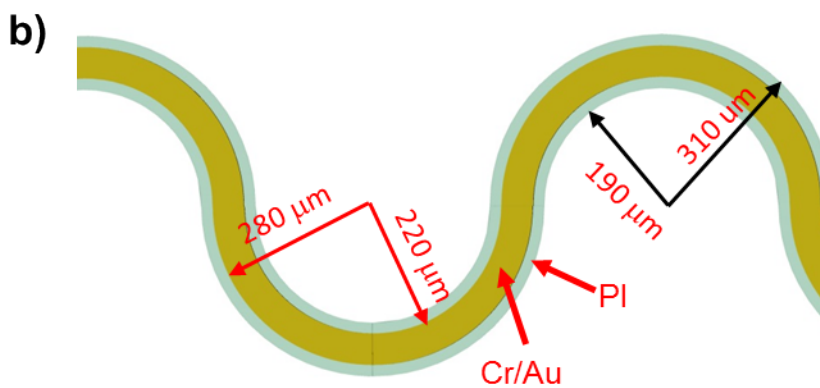
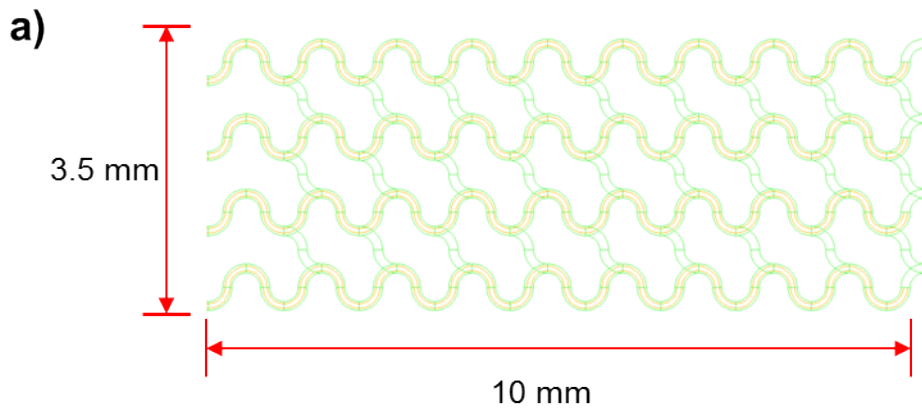
## **VI. Control group of macro-scale PAAM gel**

The fabrication of the control groups are the same as described in Section 2.4. However, instead of using PAA gels in the bottom, we used PAAM gel. In the control groups, we applied ORR at -1.15 V (vs. Au) for 30 mins and then stopped the ORR to observe the gel for another 30 mins. As shown in Fig. S6a-c, neither applying nor removing the ORR caused any significant change in the PAAM gel.. The movie of applying and removing voltage to PAAM gel is shown in S.I. Movie S5 and S6, respectively, and Fig. S6d is the plot of two cycles of strain change of the PAAM gel, which indicates that PAAM gel has no response to this pH gradient. However, Fig. 5a-c shows a clear swell-deswell transition of the PAA gel. The plot in Fig. 5d indicates a small, yet fully reversible strain change of the macro PAA gel corresponding to the application and removal of ORR.

## VII. Supplementary Information figures

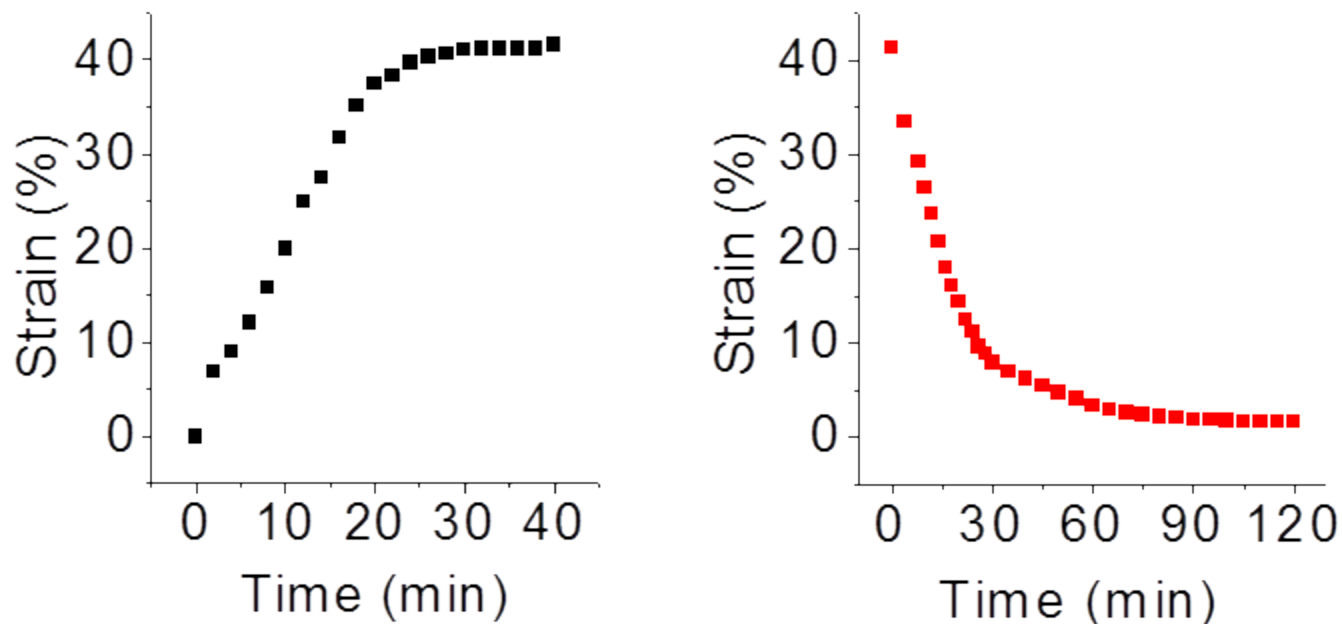


**S. Figure S1:** CV of two electrode system using Au electrode (black line) and a standard three electrode system with Ag/AgCl as reference electrode (red line). The CV indicates that the Au electrode may be utilized as a pseudo-reference electrode with a potential shift of  $\sim -0.95$  V from Ag/AgCl.

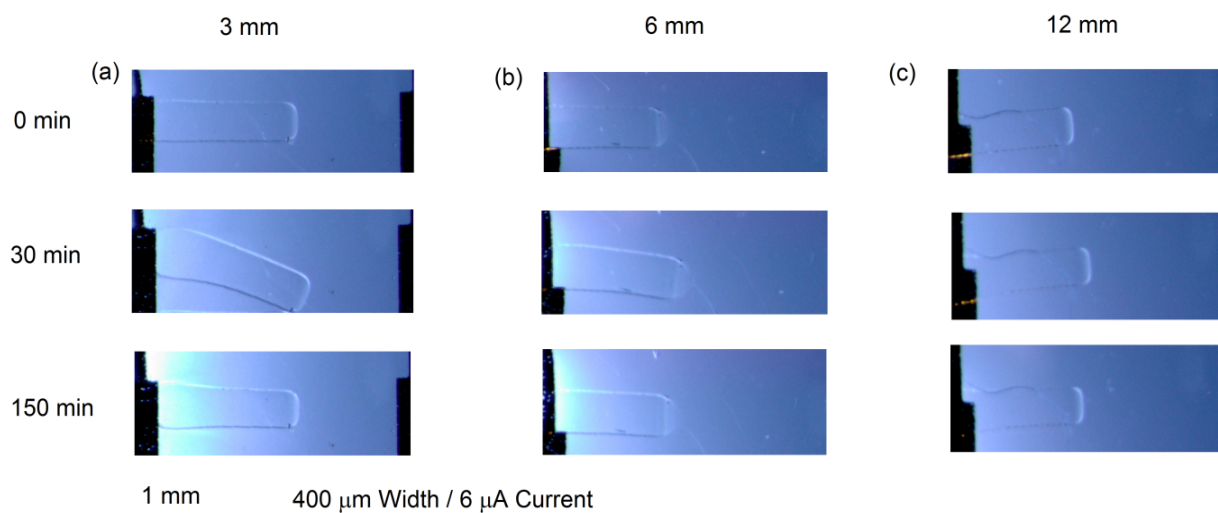


**S. Figure S2:** (a) Design of a stretchable/compressible electronic mesh. The line spacing for each electrode strain is 1 mm, yield overall dimension of 3.5 mm x 10 mm. (b) Detailed planar dimensions of the mesh, including the PI layers and metal parts: the metal arch has outer radius  $R=0.28$  mm, inner radius  $r=0.22$  mm. The PI layer is 0.02 mm wider than the metal part on both side, hence  $R_{PI}=0.30$  mm,  $r_{PI}=0.20$  mm. (c) (i) Schematic cross sectional illustration of the

mesh, including 5/400 nm Cr/Au sandwiched by two layers of 2.5  $\mu\text{m}$  PI and (ii) schematic cross sectional illustration of the mesh after completion of etching of the polyimide.

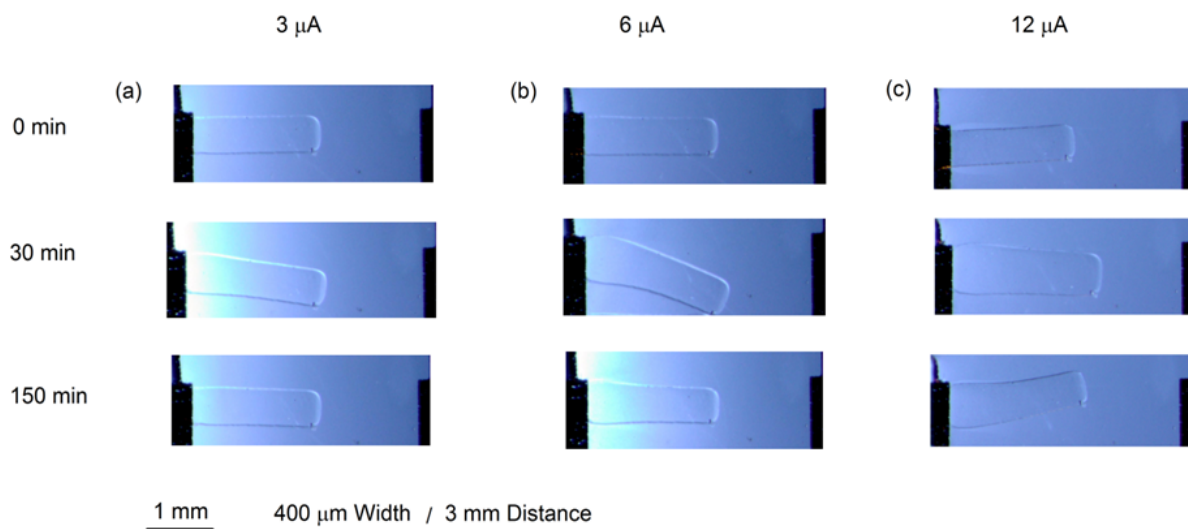


**S. Figure S3:** (a) Strain change of the PAA micro stripe while applying the ORR at  $V=-1.15\text{V}$ . (b) Strain change of the PAA micro stripe after the potential was removed from the system.

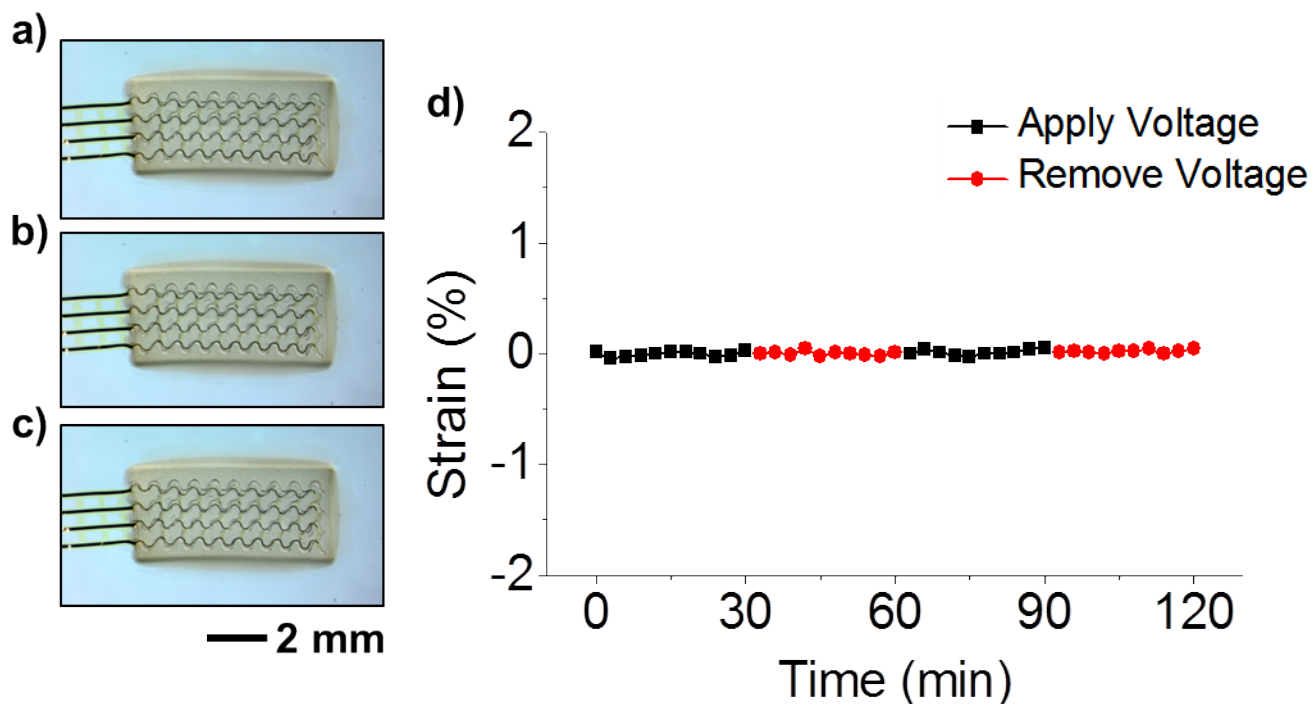


**S. Figure S4:** Pictures of the micro PAA stripe while applying ORR (0-30 mins) and after halting ORR (30-150 mins) with fixed gel width (400  $\mu\text{m}$ ) and current magnitude (6  $\mu\text{A}$ ) (a) electrode distance = 3 mm; (b) electrode distance = 6 mm; (c) electrode distance = 12 mm.





**S. Figure S5:** Pictures of the micro PAA stripe while applying ORR (0-30 mins) and after halting ORR (30-150 mins) with fixed gel width (400  $\mu\text{m}$ ) and inter-electrode distance (3 mm) (a) current magnitude = 3  $\mu\text{A}$ ; (b) current magnitude = 6  $\mu\text{A}$ ; (c) current magnitude = 12  $\mu\text{A}$ .



**S. Figure S6:** Performance of macro PAAM gel during the electrochemically catalyzed ORR reaction (a) PAAM gel slab at original electrolyte solution (0.1 M KCl, pH=4.0). (b) PAAM gel slab after 30 mins of applied ORR. (c) PAAM gel slab after ORR has been stopped for 30 min. (d) Strain change of the PAAM gel during and after the applied ORR.

## VIII. Supplementary Information movie captions

**S.I. Movie 1:** The expansion of the PAA micro stripes after applying ORR. The time span of the video is 30 minutes, and the dimension of the screen is 4.5mm x 6 mm (Height x Length).

**S.I. Movie 2:** The restoration of the PAA micro stripes after the removal of ORR. The time span of the video is 60 minutes and the dimension of the screen is 4.5mm x 6 mm (Height x Length).

**S.I. Movie 3:** The expansion of the PAA macro stripes after applying ORR. The time span of the video is 30 minutes, and the dimension of the screen is 13.5mm x 18 mm (Height x Length).

**S.I. Movie 4:** The restoration of the PAA macro stripes after the removal of ORR. The time span of the video is 30 minutes and the dimension of the screen is 13.5 mm x 18 mm (Height x Length).

**S.I. Movie 5:** The expansion of the PAAM macro stripes after applying ORR. The time span of the video is 30 minutes, and the dimension of the screen is 13.5mm x 18 mm (Height x Length).

**S.I. Movie 6:** The restoration of the PAAM macro stripes after the removal of ORR. The time span of the video is 30 minutes and the dimension of the screen is 13.5 mm x 18 mm (Height x Length).

**Reference:**

(1) Erickson, E. M.; Mitrovski, S. M.; Gewirth, A. A.; Nuzzo, R. G.: Optimization of a permeation-based microfluidic direct formic acid fuel cell (DFAFC). *Electrophoresis* **2011**, *32*, 947-956.